1st International Conference on Women Development in Engineering, Science & Technology (WD-EST'23)

03-05 October 2023

Enhancing Model Validity by Comparative Analysis of Adams-Moulton, Runge-Kutta and Euler Methods in Lengyel-Epstein Reaction Simulation for Zinc Oxide Nanostructures

Kaniz Fatima[1,*], Basit Ali[2], Mahnoor[3]

[1]*Department of Humanities and Social Sciences, Bahria University Karachi, Karachi, Pakistan.*

[2]*Department of Electrical Engineering, Bahria University Karachi, Karachi, Pakistan.*

[3]*Dow College of Pharmacy, Dow University of Health Sciences, Karachi, Pakistan.*

[*]Corresponding author email: kanizfatima.bukc@bahria.edu.com

ABSTRACT This paper examines the reaction kinematics of zinc oxide (ZnO) nanostructure formation using the Lengyel-Epstein reaction model with three distinct numerical approaches: Euler, fourth-order Runge-Kutta, and Adams-Bashforth-Moulton. The purpose of this research is to determine the optimum approximation method for calculating zinc ion (Zn^{+2}) and hydroxyl ion (OH^{-}) concentrations. In terms of accuracy, stability and consistency, the results reveal that the Adams-Bashforth-Moulton method outperforms the Euler and fourth-order Runge-Kutta techniques. It also gives a comparison with Euler's approach and fourth-order Runge-Kutta by simulating it, demonstrating that the rate of convergence of Adams-Bashforth-Moulton method is more appropriate than Euler's method and fourth-order Runge-Kutta methods. The error analysis using simulation results concluded that Adams-Bashforth-Moulton gives optimized results in comparison with Euler and Runge-Kutta methods. The Adams-Bashforth-Moulton method also validates the experimental output for the formation of zinc oxide nanostructures in the aqueous chemical growth method.

Keywords: *Lengyel Epstein, Euler, fourth-order Runge-Kutta, Adams Moulton, Nanostructures*

1. Introduction

Zinc Oxide (ZnO), a fundamental inorganic chemical, has a surprising versatility that resonates across a range of technological applications, forging an enduring role in the modern world. ZnO, distinguished by its characteristic white powdered form that defies water solubility, quickly dissolves in diluted acids and bases. ZnO nanoparticles have outstanding physical and chemical properties due to their small particle size of less than 100 nm, which distinguishes them from other metal oxides. This distinguishing feature makes ZnO a vital component in a wide range of industries, including glass and paint, optical materials, rubber, plastics, batteries, coatings, and even cosmetics. [1].

ZnO nanoparticles are emerging as essential participants in the biomedical arena, notably in the dynamic sectors of anticancer and antibacterial therapies. ZnO's unique ability to create reactive oxygen species (ROS) and release zinc ions highlights its potential as a powerful therapeutic agent. ZnO nanoparticles have the potential to improve diabetes treatment due to zinc's ability to modulate insulin levels [2, 3].ZnO's multifarious nature is rooted in its inherent semi conductivity, which endows it with properties such as electric conductivity, photosensitivity, chemical sensing, and piezoelectricity. ZnO nanoparticles are luminous even at ambient temperature and have a strong excitonic binding energy with a band gap spanning 3.4 to 3.7 eV [4]. This particular band gap is reflected in ZnO's position as a powerful UV absorber, making it a desirable component in sunscreens, skin lotions, and even wound-healing ointments. Aside from their medicinal benefits, ZnO nanoparticles have the potential to be used as drug delivery carriers due to their high biocompatibility, which has been certified by the US Food and Drug Administration (FDA) [5,6]. Among the numerous uses, the critical need for large-scale ZnO nanoparticle manufacturing stands out as a critical factor. Because of its effectiveness and versatility, the aqueous chemical growth (ACG) methodology stands out among low-temperature synthesis techniques. The ACG method's rigorous management of growth conditions enables the creation of a wide range of ZnO nanostructures, from nanorods and nanotubes to nanowires and nanospheres [7]. Because of their extraordinary properties, zinc oxide (ZnO) nanostructures such as nanorods, nanotubes, nanowires, nanoflexes, nanospheres, and nanoneedles have attracted a lot of attention. These benefits include their low cost, lack of toxicity, simplicity of manufacture, outstanding biocompatibility, high electron transfer rates, and enhanced analytical capabilities. These various ZnO morphologies are achieved by optimizing growing parameters. [8-10]

In the realm of mathematical modeling, the renowned Lengyel-Epstein reaction model plays a critical role in deciphering the complicated dynamics behind ZnO nanostructure formation [11]. Euler's approach has traditionally been used to forecast growth dynamics within this model. In light of this, this research takes a novel turn, proposing an upgraded methodology that smoothly merges Euler's method and fourth-order Runge-Kutta (RK) technique with Adam's Bashforth method. This novel combination of approaches aims to not only improve the precision and durability of the modeling process but also to understand the complicated dynamics driving the evolution of Zn ion and hydroxyl ion concentrations. This innovative technique, which combines the established and the avant-garde, aims to improve our understanding of ZnO nanoparticle

growth dynamics, therefore providing a solid bridge between theoretical ideas and empirical findings.

2. Methods

2.1. Experimental procedure

To synthesize ZnO nanoparticles, the upkeep of a controlled environment is basic due to the characteristic helplessness of the Aqueous Chemical Growth (ACG) strategy to barometrical impacts. In this strategy, a flawless gold-coated glass substrate is utilized to play down contaminants. Sometime recently commencing the method, the gold-coated glass substrate is submerged in an arrangement of low-concentration hydrofluoric corrosive. Hence, an intensive cleansing with acetone results, taken after by substrate drying utilizing nitrogen gas at encompassing temperature. With the basis laid, the substantive prepare unfurls, started by implies of the spin-coating strategy. Utilizing rotational speeds of 4500 revolutions per minute, a solution of Zinc acetate dihydrate is applied to the substrate through numerous cycles of spin coating. Post-application, the substrate is subjected to a temperature of 70°C, advancing the stabilization of the solution [11].

In the meantime, a solution is methodically prepared in a container by fusing Zinc Nitrate and hexamethylenetetramine in a 1:1 ratio. This mixture is dissolved in 250 ml of deionized water, resulting in a prepared solution. The pre-coated substrate is then immersed in the prepared solution using a specified holder. Following this immersion, the container is placed in a preheated oven set to 100°C, where it will remain for 7 hours. Following the synthesis phase, the oven is turned off for 30 minutes to allow for cooling. The substrate is detached from the holder at the end of this procedure. The end outcome is the appearance of a layer of ZnO nanorods [12-14].

A transformational evolution happens when the pH of the solution is regulated by the addition of 25% ammonia solution. This pH manipulation causes the formation of zinc oxide nanowires, which broadens and diversifies the scope and variety of the synthesized nanostructures. Two ions are required for the production of ZnO. The first is zinc ion ($Zn^{(+2)}$), whereas the second is hydroxyl ion (OH^-). After the disintegration of zinc nitrate, $Zn^{(+2)}$ may be produced from metal salt. [15]

$$Zn(NO_3)_2.6H_2O + 6H_2O \rightarrow Zn^{+2} + 2NO_3^- \quad (1)$$

After the hydrothermal breakdown of HMT, OH^- may occur.

$$(CH_2)_6N_4 + 6H_2O \rightarrow 6HCHO + 4NH_3 \quad (2)$$

$$NH_3 + H_2O \rightarrow NH_4 + OH^- \quad (3)$$

ZnO can be produced after the deposition of both ions.

$$2OH^- + Zn^{+2} \rightarrow Zn(OH)_2 \quad (4)$$

$$Zn(OH)_2 \rightarrow ZnO\ (s)\ +\ H_2O \quad (5)$$

2.2. Mathematical model

A mathematical model may also be used to illustrate the rate of growing the zinc ion Zn^{+2} and Hydroxide ion OH^- concentrations that are needed for the synthesis of ZnO [4]. The Lengyel-Epstein reaction model is applied for this. Euler's method and Runge-Kutta fourth order method are implemented as a numerical method in this model to approximate the results in the reference [11]. The Adam's Bashforth method is now employed in this study to estimate the increase of zinc ion and hydroxyl ion. The following equations were used to build the model:

$$NH_3 + H_2O \rightarrow NH_4^+ + OH^- \quad (6)$$

$$Zn(NO_3)_2.6H_2O + 6H_2O \rightarrow Zn^{+2} + 2NO_3^- \quad (7)$$

$$2OH^- + Zn^{+2} \rightarrow ZnO + H_2O \quad (8)$$

The differential equations derived in [11] using the Lengyel-Epstein reaction model are as follows: where x and y indicate the concentrations of $OH^-$and Zn^{+2} respectively.

$$\frac{dx}{dt} = f(x,y) = a_1 - x - 4\left(\frac{xy}{(1+x^2)}\right) \quad (9)$$

$$\frac{dy}{dt} = g(x,y) = a_2 x\left(1 - \frac{y}{(1+x^2)}\right) \quad (10)$$

The suggested differential equations were built using the theory presented by Carmen Chicone in [16]. The differential equations above are affected by the values of a_1 and a_2. To calculate the steady-state concentrations, use $a_2 > \frac{3a_1}{5} - \frac{25}{a_1}$. The experimental development of ZnO was observed to end at a given time period and to exhibit linear behavior [17, 18]. Iterating the equations yields the estimated values of the aforementioned differential equations using the

Adam's Bashforth approach.

When solving ordinary differential equations (ODEs) numerically, there are several approaches for approximating the solution across discrete time steps. We compare the performance of three widely used methods: Euler's approach, 4th Order Runge-Kutta, and Adams-Bashforth, with an emphasis on their application to the growth kinetics study of Zinc oxide (ZnO) nanostructures.

Euler's method is a fundamental numerical approach for approximating the solution of ordinary differential equations by linearly extrapolating from the present position using the derivative. Despite its apparent simplicity, Euler's approach can result in severe inaccuracies, particularly when working with stiff equations or complex dynamics. Euler's approach may give basic insights in the context of ZnO nanostructure formation, however it is restricted in precision and accuracy.

The 4^{th} order Runge-Kutta method is the common used numerical integration method that is better than Euler's method in terms of accuracy. Four intermediary steps are required to estimation of the next point. This methodis ultimate for solving ordinary differential equations with moderate to complicated problems. Runge-Kutta gives a more accurate depiction of the behavior of the system than Euler's method when applied to the growth kinetics of ZnO nanostructures.

The Adams-Bashforth method is a numerical approach for solving ordinary differential equations by integrating a system of equations across discrete time steps. The Adams-Bashforth method is used deliberately in this study to increase the computational efficiency of the Lengyel-Epstein reaction model for the growth kinetics of Zinc oxide nanostructures. Using the Adams Bashforth Moulton method, the following processes can be used to determine the growth rate of ZnO at each time step.

The predictor step employs a fourth-order Adams-Bashforth method to predict the values of x and y at the next time step. The predictor formula for 'x' is given by:

$$x_{pred} = x_i + \frac{\Delta t}{24}(55f_i - 59f_{i-1} + 37f_{i-2} - 9f_{i-3}) \tag{11}$$

The predictor formula for 'y' is given by:

$$y_{pred} = y_i + \frac{\Delta t}{24}(55g_i - 59g_{i-1} + 37g_{i-2} - 9g_{i-3}) \tag{12}$$

Here, f_i and g_i represent the evaluated values of the rate equations at time t_i.

Using the predicted values x_{pred} and y_{pred} from the predictor step, a corrected estimate for **x** and **y** is obtained using the Adams-Moulton corrector formula:

$$x_{i+1} = x_i + \frac{\Delta t}{24}\left(9f_{pred} + 19f_i - 5f_{i-1} + f_{i-2}\right) \tag{13}$$

$$y_{i+1} = y_i + \frac{\Delta t}{24}\left(9g_{pred} + 19g_i - 5g_{i-1} + g_{i-2}\right) \tag{14}$$

The integration process continues iteratively over the specified time span, refining the values of **x** and **y** using the predicted and corrected estimates.

3. Results and Discussion

Fig. 1 illustrates the concentrations of OH^- and Zn^{+2} for the exact solution. Particularly, the minimum OH^- concentration seen at 0.38080, at the time point 1.18658 hour. Simultaneously, the maximum Zn^{+2} concentration peaks at 1.30732, occurring precisely at time 0.41048 h.

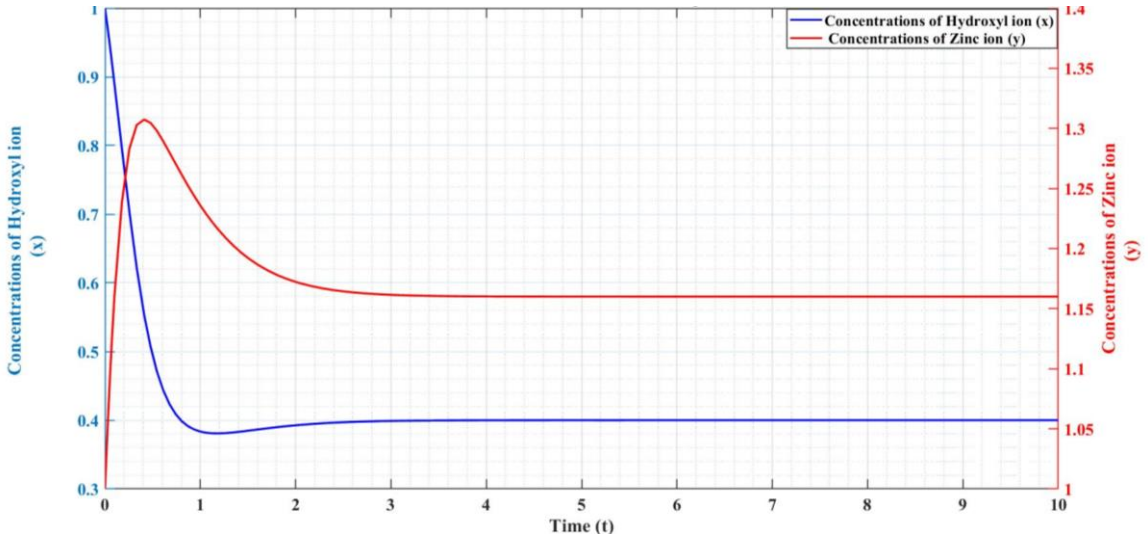

Fig. 1: Concentrations of OH^- and Zn^{+2} for the exact solution

Fig. 2 shows the concentrations of OH^- and Zn^{+2} obtained from the Euler's method. Here, the minimum OH^- concentration is lower, measuring 0.379341, also at the time 1.18658 h. The maximum Zn^{+2} concentration for Euler's method is higher, at 1.314709, occurring at the same time point of 0.41048 h.

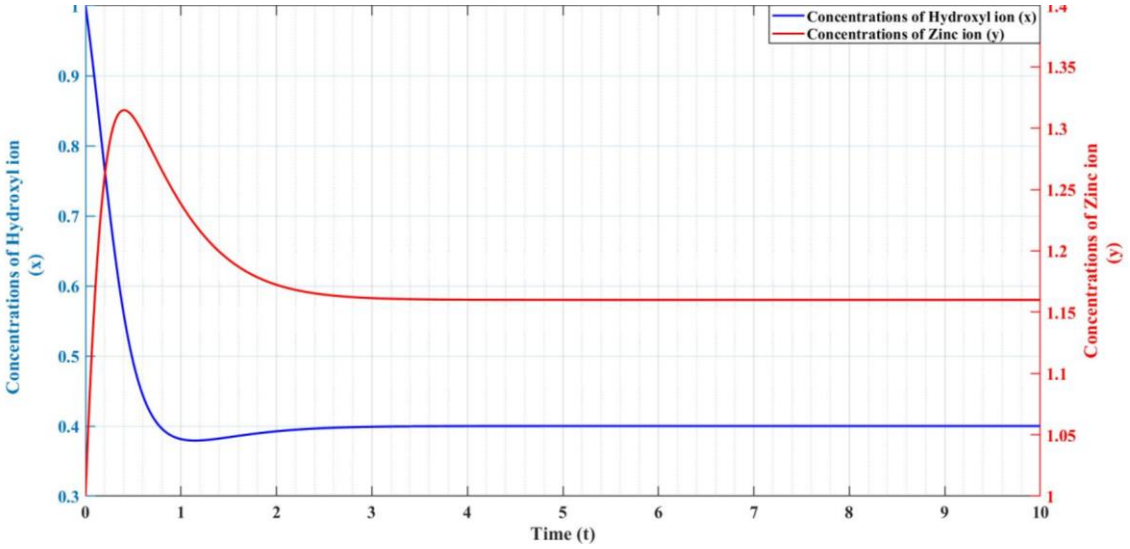

Fig. 2: Concentrations of OH^- and Zn^{+2} for Euler's method

Fig. 3 illustrates the results obtained through the 4th order Runge-Kutta method. In this method, the minimum OH^- concentration is 0.380547, close to the value of exact solution, at the time 1.18658 h. The maximum Zn^{+2} concentration for the 4th order Runge-Kutta method is 1.309011, at time 0.41048 h.

Fig. 4 presents the concentrations of OH^- and Zn^{+2} obtained from the Adams-Bashforth method. Here, the minimum OH^- concentration is 0.3806, closest to the exact solution at time 1.18658 h. While the maximum Zn^{+2} concentration for the Adams-Bashforth method is 1.30886, at time 0.41048 h. These comparisons among different methods provide valuable understandings into the accuracy, stability and performance of each method in modeling the chemical dynamics.

Table 1 provides a thorough overview of the concentrations of OH^- and Zn^{+2} determined by three different techniques: Euler's method, Runge-Kutta method of fourth order, and Adams-Bashforth method. The results produced by these various mathematical approaches can be contrasted and compared using the information in this table.

3.1. Error Analysis

When estimating OH^- and Zn^{+2} concentrations at given time points, the three numerical methods, Euler'sapproach,4th Order Runge-Kutta, and Adams-Bashforth, show significant differences in their accuracy. The largest errors for Euler's method at t=1.18658 are 0.383% error for OH^- and 0.565% error for Zn^{+2} illustrating its imprecise nature. The 4th Order Runge-Kutta method and the Adams-Bashforth method both significantly lower errors at their respective time points, with error

values for OH^- and Zn^{+2} of 0.129% and 0.118%, respectively. As a result of Adams-Bashforth's lower error rates for these concentration estimates, this research emphasizes the trade-off between a numerical approach's simplicity and accuracy.

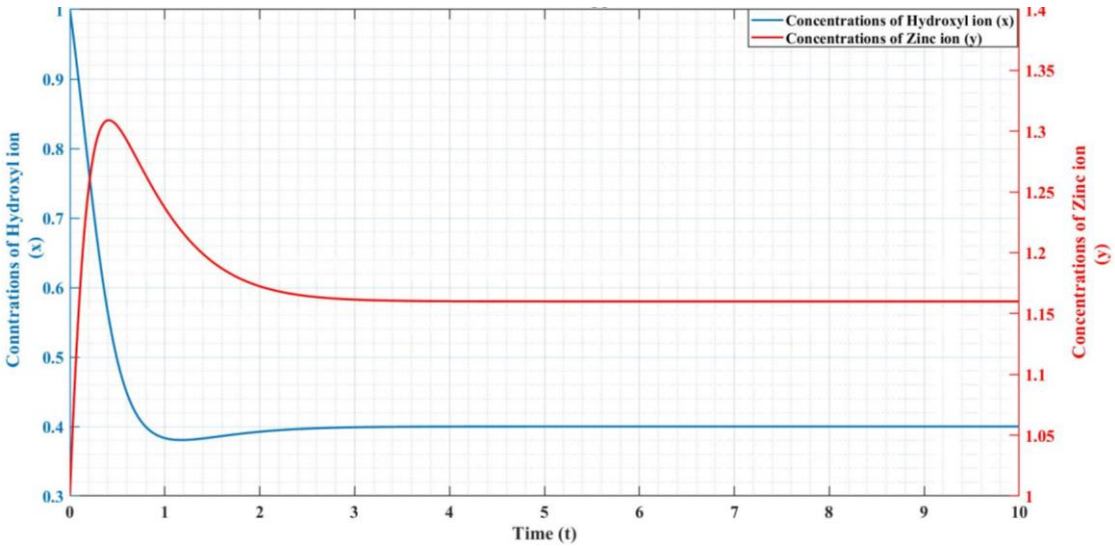

Fig. 3: Concentrations of OH^- and Zn^{+2} for RK 4th order method

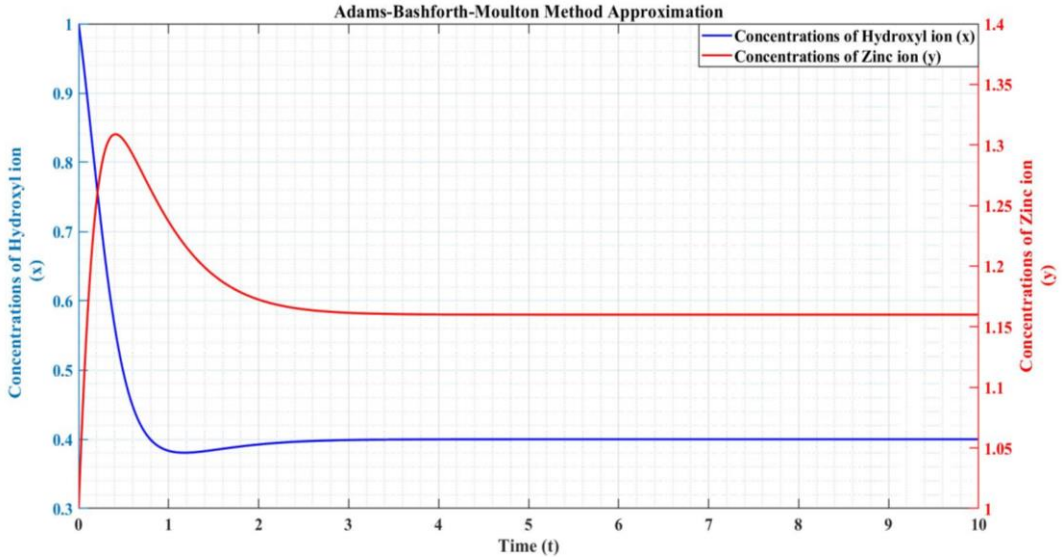

Fig. 4: Concentrations of OH^- and Zn^{+2} for Adams-Bashforth method

The error analysis for the concentrations of OH^- and Zn^{+2} using the three methods; Euler's method, Runge-Kutta method of fourth order, and Adams-Bashforth method is shown in table 2. This table provides a thorough analysis of the precision and variances of each method for

calculating these chemical concentrations, assisting in the evaluation of their individual performances. Fig. 5 depicts the error analysis for all the three numerical techniques.

Table 1: Concentrations of OH^- and Zn^{+2} for the numerical methods

	Concentrations of OH^-	Concentrations of Zn^{+2}
	For t=1.18658	For t=0.41048
Euler's method	0.379341	1.314709
4th order Runge-Kutta method	0.380547	1.309011
Adams-Bashforth method	0.3806	1.30886

Table 2: Error of the concentrations of OH^- and Zn^{+2} for the numerical methods

	Concentrations of OH^-	Concentrations of Zn^{+2}
	For t=1.18658	For t=0.41048
Euler's method	0.383%	0.565%
4th order Runge-Kutta method	0.066%	0.129%
Adams-Bashforth method	0.053%	0.118%

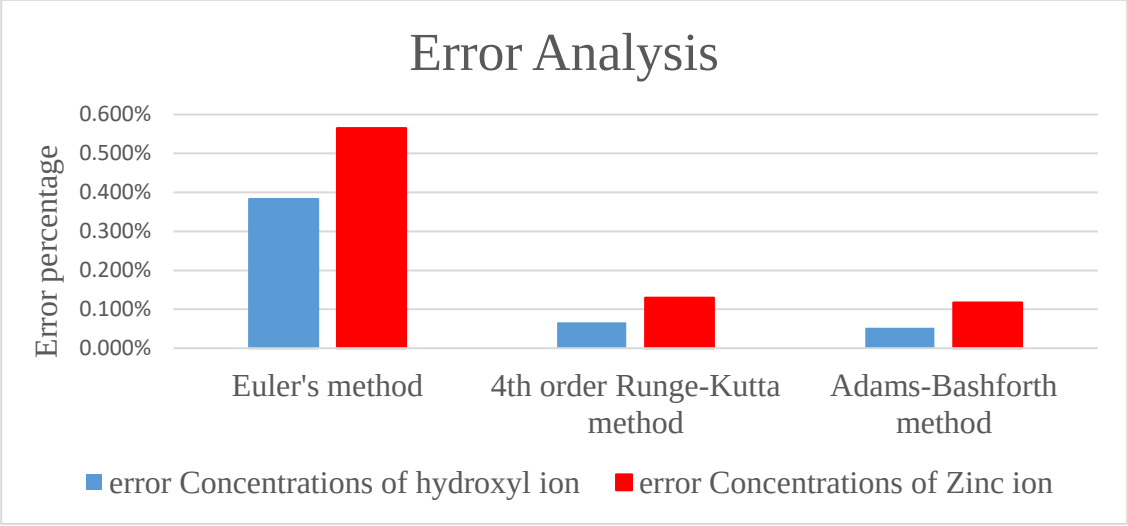

Fig. 5: Error of the concentrations of OH^- and Zn^{+2} for the numerical methods

4. Conclusion

In the realm of numerically solving ordinary differential equations (ODEs), the choice of method depends on the accuracy, computational efficiency, stability, and the complexity of the system. Euler's method is simple but less accurate, suitable for computationally efficient tasks. In contrast, 4th Order Runge-Kutta and Adams-Bashforth offer increased accuracy, with Adams-Bashforth often providing the most precise results due to its predictor and corrector steps. When dealing with complex systems like the growth kinetics of ZnO nanostructures, where subtle interactions are significant, both 4th order Runge-Kutta and Adams-Bashforth outperform Euler's method, with Adams-Bashforth standing out for its ability to capture intricate behaviors while maintaining reasonable computational efficiency.

References

[1] Siddiqi KS, Rahman AU, Tajuddin, Husen A. Properties of zinc oxide nanoparticles and their activity against microbes. Nanoscale Res Lett. 2018;13(1):1-13.
[2] Jiang J, Pi J, Cai J. The advancing of zinc oxide nanoparticles for biomedical applications. Bioinorg Chem Appl. 2018;2018:e1062562.
[3] Tang E, Cheng G, Ma X, Pang X, Zhao Q. Surface modification of zinc oxide nanoparticle by PMAA and its dispersion in aqueous system. Appl Surface Sci. 2006;252(14):5227-5232.
[4] Fatima K, Khan A, Hussain M. Mathematical modelling of reaction kinematics of one-dimensional zinc oxide nanostructures. NED Univ J Res. 2018;15(4):117-122.
[5] Mishra PK, Mishra H, Ekielski A, Talegaonkar S, Vaidya B. Zinc oxide nanoparticles: A promising nanomaterial for biomedical applications. Drug Discov. 2017;22(12):1825-1834.
[6] Sabir S, Arshad M, Chaudhari SK. Zinc oxide nanoparticles for revolutionizing agriculture: synthesis and applications. Sci World J. 2014:e925494.
[7] Osman, D. A. M., & Mustafa, M. A. (2015). Synthesis and characterization of zinc oxide nanoparticles using zinc acetate dihydrate and sodium hydroxide. J. Nanosci. Nanoeng, 1(4), 248-251.
[8] Chandiran AK, Abdi-Jalebi M, Nazeeruddin MK, Grätzel M. Analysis of electron transfer properties of ZnO and TiO2 photoanodes for dye-sensitized solar cells. ACS nano. 2014;8(3):2261-2268.
[9] Bai X, Wang L, Zong R, Lv Y, Sun Y, Zhu Y. Performance enhancement of ZnO photocatalyst via synergic effect of surface oxygen defect and graphene hybridization. Langmuir. 2013;29(9):3097-3105.
[10] Hatamie A, Khan A, Golabi M, et al. Zinc oxide nanostructure-modified textile and its application to biosensing, photocatalysis, and as antibacterial material. Langmuir. 2015;31(39):10913-10921.

[11] Fatima, K., & Ali, B. (2022). Implementation of Lengyel-Epstein Reaction Model for Zinc Oxide (ZnO) Nanostructures by Comparing Euler and Fourth-Order Runge–Kutta (RK) Methods. Scientific Inquiry and Review, 6(1).

[12] Khan A, Hussain M, Abbasi MA, Ibupoto ZH, Nur O, Willander M. Analysis of junction properties of gold–zinc oxide nanorods-based Schottky diode by means of frequency dependent electrical characterization on textile. J Mater Sci. 2014;49(9):3434-3441

[13] Qiu Y, Zhang H, Hu L, et al. Flexible piezoelectric nanogenerators based on ZnO nanorods grown on common paper substrates. Nanoscale. 2012;4(20):6568-6573.

[14] Lee CY, Wang JY, Chou Y, et al. White-light electroluminescence from ZnO nanorods/polyfluorene by solution-based growth. Nanotechnology. 2009;20(42):e425202.

[15] Greene LE, Yuhas BD, Law M, Zitoun,D, Yang P. Solution-grown zinc oxide nanowires. Inorg Chem. 2006;45(19):7535-7543. https://doi.org/10.1021/ic0601900

[16] Chicone, C. (2010). Mathematical modeling and chemical kinetics. A module on chemical kinetics for the University of Missouri Mathematics in Life Science program, 8.

[17] Caetano, B. L., Santilli, C. V., Meneau, F., Briois, V., & Pulcinelli, S. H. (2011). In situ and simultaneous UV− vis/SAXS and UV− vis/XAFS time-resolved monitoring of ZnO quantum dots formation and growth. The Journal of Physical Chemistry C, 115(11), 4404-4412.

[18] Mishra, Y. K., Modi, G., Cretu, V., Postica, V., Lupan, O., Reimer, T., ... & Adelung, R. (2015). Direct growth of freestanding ZnO tetrapod networks for multifunctional applications in photocatalysis, UV photodetection, and gas sensing. ACS applied materials & interfaces, 7(26), 14303-14316.

[19]